Title

Combinatorial Library Screening with Liposomes for Discovery of Membrane Active Peptides

Journal

ACS Combinatorial Science, 19(5)

ISSN

2156-8952

Authors

Carney, Randy P
Thillier, Yann
Kiss, Zsofia
et al.

Publication Date

2017-05-08

DOI

10.1021/acscombsci.6b00182

Peer reviewed

HHS Public Access

Author manuscript

ACS Comb Sci. Author manuscript; available in PMC 2018 April 16.

Published in final edited form as:

ACS Comb Sci. 2017 May 08; 19(5): 299–307. doi:10.1021/acscombsci.6b00182.

Combinatorial Library Screening with Liposomes for Discovery of Membrane Active Peptides

Randy P. Carney[†], **Yann Thillier**[†], **Zsofia Kiss**[†], **Amir Sahabi**[†], **Jean Carlos Heleno Campos**[†], **Alisha Knudson**[†], **Ruiwu Liu**[†], **David Olivos**[†], **Mary Saunders**[†], **Lin Tian**[†], and **Kit S. Lam**[†,‡]

[†]Department of Biochemistry and Molecular Medicine, University of California Davis, 2700 Stockton Blvd., Sacramento, CA 95817, United States

[‡]Division of Hematology/Oncology, University of California Davis Cancer Center, Sacramento, CA, USA

Abstract

Membrane active peptides (MAPs) represent a class of short biomolecules that have shown great promise in facilitating intracellular delivery without disrupting cellular plasma membranes. Yet their clinical application has been stalled by numerous factors: off-target delivery, a requirement for high local concentration near cells of interest, degradation en route to the target site, and, in the case of cell-penetrating peptides, eventual entrapment in endolysosomal compartments. The current method of deriving MAPs from naturally occurring proteins has restricted the discovery of new peptides that may overcome these limitations. Here we describe a new branch of assays featuring high-throughput functional screening capable of discovering new peptides with tailored cell uptake and endosomal escape capabilities. The one-bead-one-compound (OBOC) combinatorial method is used to screen libraries containing millions of potential MAPs for binding to synthetic liposomes, which can be adapted to mimic various aspects of limiting membranes. By incorporating unnatural and *D*-amino acids in the library, in addition to varying buffer conditions and liposome compositions, we have identified several new highly potent MAPs that improve on current standards and introduce motifs that were previously unknown or considered unsuitable. Since small variations in pH and lipid composition can be controlled during screening, peptides discovered using this methodology could aid researchers building drug delivery platforms with unique requirements, such as targeted intracellular localization.

Correspondence to: Randy P. Carney; Kit S. Lam.

Associated Content

Supporting Information

Containing a full description of materials and experimental methods. This material is available free of charge via the Internet at http://pubs.acs.org.

Author Contributions

R.P.C. and K.S.L. conceived and designed the experiments, R.P.C., Y.T., Z.K, A.S., J.C.H.C., and A.K performed the experiments. R.L. sequenced the positives hits and developed the chemical procedures. D.O., M.S., and L.T. conceived and developed the automated library screening procedure and custom software. R.P.C. composed the manuscript. All authors have given approval to the final version of the manuscript.

The authors declare no competing financial interests.

Introduction

The current landscape of delivery agents for gene therapy, particularly for treating cancer, is plagued by numerous limitations: quick degradation in the blood, cellular toxicity, and most critically, an inability to overcome intracellular barriers, such as poor cell membrane penetration or endosomal escape.[1,2] To address these issues and perform efficient, targeted drug delivery, intense study is underway for the application of novel biomaterials, including nanoparticles, polymers, gels, and other diverse nanoformulations.[3] Tools used to study interactions with synthetic membranes are increasingly useful for steering the development of effective medications that traverse intracellular barriers. Here we outline the proof of concept for a high-throughput screening platform for testing of hundreds of thousands of peptides for their interactions against lipid vesicles of various compositions under different conditions such as pHs. We believe further studies in this direction will facilitate the understanding of peptide-membrane interactions and the development and characterization of new cell-penetrating peptides (CPPs) and endosomolytic peptides, or more broadly, membrane active peptides (MAPs).[4]

More than 1,800 putative CPPs have been reported in the literature, yet there is little parity in reporting the mechanisms of peptide-membrane interaction.[5] While their ability to chaperone therapeutic cargo (e.g. peptides, proteins, genes, small molecule drugs, quantum dots, nanoparticles) across the cell membranes has been extensively reviewed,[6] CPPs have not seen widespread clinical application. In fact, the majority used for drug delivery are cationic and their cell uptake requires high local concentration, two interdependent factors that generally impart cellular toxicity.[6] However, recent studies have indicated that the presumed requirement for cationicity is directly related to achieving a necessary threshold CPP concentration at the anionic cell surface, and unrelated to the subsequent mechanisms of membrane insertion/penetration,[7] and some new anionic CPPs have indeed been reported.[5,7,8]

As one recent study highlights, there is an imminent need for high-throughput approaches to MAP discovery and characterization.[9] The one-bead-one-compound (OBOC) combinatorial library method is one such approach that affords the following advantages: (i) the high number of possible hits allows for classification of motifs in peptide sequence associated with membrane activity, aiding in the elucidation of mechanisms that are currently poorly defined, (ii) vesicle composition (lipids, cholesterol content, membrane proteins) and buffer conditions can be built into the screening conditions to better mimic various stages of the endosomal pathway, and (iii) inclusion of unnatural, *D*- and *β*-amino acids can overcome limitations of quick degradation, immunogenicity, and low membrane permeability associated with peptides made of natural amino acids (e.g. recognition by degradative enzymes or the sterically-dependent MHC-antigen T-cell receptor).[10] There has been some success in applying combinatorial techniques to peptide discovery,[11–13] but none have approached the potential throughput of the OBOC screening presented here. In the OBOC methodology, each polymer microbead displays a unique peptide, leading to a library of millions potential MAPs via a combinatorial chemistry approach. For the discovery of cell-type specific membrane targets, living cells are typically used as probes to screen the bead libraries for cell binding.[14,15] Here we screen OBOC peptide libraries for beads that

exhibited strong binding to synthetic liposomes with defined size, lipid composition and at different pHs that simulate specific limiting biomembranes. Our central hypothesis is that MAPs can be found by screening combinatorial libraries against the desired type of membrane, e.g. CPPs could be found by screening against ”cell membrane-type” vesicles, and pH dependent MAPs (pMAPs) can be discovered by screening ”endosomal-type” vesicles under acidified pH conditions (Figure 1).

Results

CPP screening and library design

OBOC combinatorial peptide libraries (7 to 9-mers) were prepared with standard solid phase peptide synthesis method using 90 μm TentaGel beads (polystyrene beads grafted with PEG) and Fmoc-chemistry. According to CPPSite, an online database of reported CPPs, roughly 20% of known CPP sequences are within this size range.[5] Screening was performed under confocal laser scanning microscopy (CLSM) by handpicking beads visibly verified to bind a critical number of fluorescently-labeled intact vesicles at the bead surface (Fig. 2a,b). For screening, the OBOC library was temporarily immobilized on planar polystyrene surface (e.g. Petri dish) with 90% (vol/vol) dimethylformamide (DMF) in dichloromethane (DCM) and imaged under CLSM with automated tile-scanning. Hndreds of thousands of beads can be screened within 20 mins, and change in fluorescence for each bead can be quantified and ranked using custom-written Matlab software. Bead immobilization enables sequential screening of the entire library under various conditions (e.g. pH, ionic strength) and with liposomes of different compositions, while at the same time enabling tracking of each and every bead during the screening process. Ethanol was be used to remove bound vesicles between screening conditions.

We chose the building blocks for a test OBOC peptide library from a large pool of L-amino acids, D-amino acids, unnatural amino acids, lipids, organic molecules, etc., with regard to functional groups typical of known MAPs, including TAT, transportan, penetratin, and INF-7, each initially derived from HIV-1 Tat, the neuropeptide galanin, the Antennapedia homeoprotein, and the inuenza virus hemagglutinin protein, respectively. Various anionic, cationic, polar uncharged, and nonpolar residues were incorporated in the library, and certain residues known to comprise MAPs (i.e. arginine, proline, acidic residues) were weighted higher. Polyarginines (e.g. R8, R9) have been heavily correlated to cell penetration effectiveness, due to their triggering of endocytosis upon binding to cell surface heparan sulfate proteoglycans.[16] Proline-rich amphipathic peptides have also been identified as potent, non-toxic CPPs.[17] Increased protonation of acidic residues (e.g. glutamic acid) in low pH endosomal compartments generally increases the peptide’s hydrophobic character, leading to fusion and eventual disruption of the endosomal membrane, which effectively releases the endosomal contents into the cytoplasm. The full table of residues comprising the library in Figure 3c.

In the most basic implementation of vesicle screening, beads in suspension were incubated with fluorescently-labeled giant unilamellar vesicles (GUVs) for 2 h, vigorously washed to remove non-binding liposomes, and examined under CLSM for positive hits. Zwitterionic giant unilamellar vesicles (GUVs) were chosen for our initial experiments because: (i)

electrostatic binding of vesicles to beads with charged peptides may occur with net cationic/anionic lipids, (ii) GUVs are large enough for visible identification of lamellar structure under CLSM, in order to ensure that vesicles were intact during binding (such that screen did not select for binding to individual fluorescent lipids), and (iii) the ease of GUV electroformation allows for the quick (~hours), robust synthesis of large numbers of GUVs with mixed lipid content (Supporting Figure S1). Zwitterionic GUVs were composed of 99% zwitterionic lipid: 1,2-dioleoyl-sn-glycero-3-phosphocholine (DOPC), and 1% fluorescent lipid: 1,2-dipalmitoyl-sn-glycero-3-phosphoethanolamine-N-lissamine rhodamine B sulfonyl, ammonium salt (Rhod-PE).

To evaluate GUV binding to library beads, we quantified change in fluorescence over time, rather than end-point fluorescence. This is preferred for several reasons: first, given that beads exhibit some sequence-specific autofluorescence that is not constant across beads, we find the change in fluorescence to be a more reliable indicator for liposome binding. In order to track each bead over the duration of several binding assays featuring different conditions, we start by scanning the fixed beads alone as a starting point. Every bead autofluoresces to some extent in the green channel, thus this channel was used to simply track the beads' locations across conditions (Figure 2c). The red channel was used to quantify differences in fluorescence for each bead according to GUV binding, and normalized by any autofluorescence measured during the control screen (no GUVs). The advantage of this approach is subtle: by screening the beads prior to GUV addition under conditions of increased laser gain, we are more sensitive to changes in fluorescence occurring as a result of GUV binding. However, this increased gain results in the generation of increased autofluorescence in the red channel for a number of given beads. By normalizing changes in fluorescence to the first control screen without GUVs, any autofluorescence can be corrected for.

After three rounds of screening with increasing stringency for the number of bound GUVs (reducing incubation time by 30 mins per cycle), the best five sequences were isolated out of 68,921 beads (<0.01%) selected randomly from the 7 to 9-mer peptide OBOC library, and sequenced on an automated protein microsequencer. Given that their primary discerning factor is *bi*nding *lip*osomes, we named these new peptides bLips, thus assigned the five beads an alphanumerical code: bLip1–5. Each of the five bLips discovered in this screen exhibit strong amphiphilic nature typical of MAPs (Fig. 3a), yet certain other features were unexpected, such as anionic/zwitterionic character and the high occurrence of unnatural amino acids like homocitrulline (HoCit - featuring a urea-type functional group) and small hydrophobic residues (amino acids with side chains of cyclopropane - Acpc, and isobutane - Aib). These residues have not been reported for any known MAP, and were subsequently investigated for cell uptake behavior.

Cell uptake and toxicity

When re-synthesized in solution form and covalently attached to a fluorescent dye (5-Carboxytetramethylrhodamine, or TAMRA) for tracking cell internalization, all five bLips (found to binding zwitterionic GUVs on beads) showed quick cellular uptake within 30 minutes (30 μM incubation concentration). The best peptide, bLip5, showed very high

uptake in many types of cells, including A549 lung adenocarcinoma and ES2 ovarian carcinoma cells (Fig. 4). Although preliminary, this experiment shows the efficacy of our screening approach; indeed it is possible to reliably observe vesicle-bound beads in a high-throughput fashion (dozens of library beads bound vesicles out of the hundreds screened), and that strong evidence supports a link between liposomal binding and *in vitro* cell uptake.

In order to contextualize the cell uptake efficiency of the bLips discovered by OBOC library screening, we compared our best CPP, bLip5, with nona-arginine (R9), which is typically cited as one of the most efficacious CPPs.[18] Both bLip5 and R9 were functionalized with a single TAMRA dye moiety via a short PEG spacer at the peptide's N-terminus. R9-TAMRA and bLip5-TAMRA were each incubated at a final concentration of 5 μM with A549 cells for 30 min (thus more stringent than our previous cell uptake experiments) before washing, staining cell nuclei, and imaging by CLSM (Figure 5a). By quantifying the magnitude of fluorescence normalized by total cell area, we observed that R9-TAMRA outperformed bLip5 by nearly two-fold fluorescence intensity increase. This finding indicates that while exhibiting CPP character, the lead bLips found in this study did not exceed or even match the excellent uptake of R9.

Given that the peptide bLips did show moderate cell uptake and thus have potential for biological applications, their cell toxicity was investigated and compared to nona-arginine (R9). R9 is typically cited as one of the most efficacious CPPs, but imparts some cellular toxicity, limiting its *in vivo* application.[18] bLips and R9 were incubated from low to high concentration (5, 30, 100 μM) with A549 cells for 3 hours before washing and viability analysis performed using flow cytometry. Propidium iodide (PI) was used to probe viability, since those cells taking up PI within a few minutes of addition exhibit cell membrane leakage from apoptosis. Representative fluorescence distributions and the percentage of viable cells following peptide incubation are presented in Figure 6. We found that bLips1–5 impart only little cell toxicity compared to R9, even at increased molar concentration.

Sequential library screening

Given the observed correlation between on-bead peptide/vesicle binding and *in vitro* cell uptake, we conceived a series of sequential OBOC library screening with liposomes of various compositions, and at different buffer pH conditions, that were built to mimic different cellular compartments. According to reported average compositions for eukaryotic cells,[19] we synthesized two unique types of GUVs, either reflecting the composition of the plasma membrane (PM-GUVs) or instead the late endosomal compartment (LE-GUVs). PM-GUVs were composed of 40% DOPC, 25% 1,2-dioleoyl-sn-glycero-3-phosphoethanolamine (DOPE), 10% 1,2-dioleoyl-sn-glycero-3-phospho-L-serine (DOPS), and 25% sphingomyelin (SM), with a cholesterol/phospholipid molar ratio of 1 (all percents represent molar ratios). LE-GUVs were slightly depleted of SM, anionic DOPS, and cholesterol, but featured an additional LE-rich molecule, bis(monoacylglycero)phosphate (BMP).[19] Therefore LE-GUVs were composed of 50% DOPC, 24% DOPE, 1% DOPS, 10% sphingomyelin, and 15% BMP, with a cholesterol/phospholipid molar ratio of 0.5. Both lipid formulations featured 1% of the Rhod-PE lipid for fluorescent labeling. PM- and LE-GUVs were screened under pH conditions appropriate to their cellular locale, thus neutral (pH =

7.4) for PM-GUVs, and more acidic (pH = 5.5) for LE-GUVs. 157,423 beads were analyzed for binding across the two conditions. The top 4 peptides that bound to (i) PM-GUVs at pH = 7.4, (ii) LE-GUVs at pH = 5.5, or (iii) both, were sequenced (Fig. 3b). Each of the new bLips (named bLip6–9) were first imaged by CLSM for cell uptake in A549 tumor cells (Fig 7) in identical conditions to the previous bLips1–5.

GUV binding controls

Control beads devoid of peptide functionalization were used to determine the extent of non-specific GUV binding. In the case of incubation with zwitterionic GUVs, no beads were observed to significantly adsorb vesicles after replacing the solution with fresh PBS twice. For anionic PM-GUVs and LE-GUVs, some beads (<1%) were observed to adsorb GUVs, but only to a minor extent (Supporting Figure S2b). This is unsurprising considering the cationic amine groups decorating the naked beads' surfaces. Yet even those beads could be stripped by more stringent washing in ionic buffer (PBS). Thus throughout the study, we employed the washing necessary to strip GUVs from naked beads, namely four solution replacements, each accompanied by a few seconds of gentle agitation. We reason that the lipid headgroups comprising the surface of the GUVs largely resist non-specific adsorption to the beads, given that they primarily interact with the bead's PEGylated exterior surface. To further ensure that beads exhibiting a low background of non-specific adsorption (i.e. false positives) were not chosen, we limited chosen beads to only the best binding ones (brightest by fluorescence). Therefore, for example in the sequential library screen, we only chose 22 beads out of 157,423 (~0.01%) that were distinctly separated from the rest with regards to fluorescence intensity change (Figure 2e). Even without washing, this level of binding was not observed in any control beads. Due to the stringency of our sequential screening methodology and the fact that we only took the top ~0.01% brightest beads, we likely eliminated the majority of false positives. Yet it is possible that false negatives (i.e. library compounds that exhibit membrane activity in solution, but do not bind liposomes) do exist and are missed by our screen. Therefore, while this screening methodology is suitable to discover certain cell penetrating or endosomolytic peptides, it can not be considered a catch-all for MAPs in general.

An additional issue is that solid phase bead scaffolds are not always chemically or physically uniform, and on occasion beads were observed that were clearly cracked or otherwise defunct, sometimes accompanied by large amounts of red fluorescence. These beads were easily avoided during automated screening since we could check the images of each positive hit and remove any beads containing obvious artifacts (Supporting Figure S2c, white arrow). Furthermore, the large size of the GUVs aids in this task, as the pattern of fluorescence for bound GUVs was quite characteristic due to their noticeable curvature. To further confirm that bead uniformity did not lead to false positives or otherwise confounding results, several bLips were resynthesized on beads to create a control experiment where every bead is coated with the same peptide. Following GUV binding (while matching the screening conditions to the original ones used for their discovery), we observed the beads to retain their respective GUV binding. Furthermore, each bead coated with the same bLip exhibited a markedly similar pattern of fluorescence (Supporting Figure S2). Finally, R9 was synthesized on TG beads in order to compare its GUV binding capabilities to the bLips discovered here. We

observed some binding to the R9 beads with PM-GUVs, but none with LE-GUVs. This finding fits with our experimental interpretations, as R9 is known to exhibit CPP behavior, but not to promote endosomolysis. However, we previously measured R9-TAMRA to be a potent cell-penetrating agent that is at least twice as efficient as the best CPP (bLip5) found by OBOC GUV screening, yet on bead, both R9 and bLip5 bound GUVs to the same extent. This suggesting that the extent of liposome binding (i.e. magnitude of fluorescence) may not be a suitable proxy for cell uptake efficiency.

One final issue that was not addressed here is the effect of peptide density on the surface of the beads. It is possible in these experiments that the particular hits discovered were directly influenced by the degree of peptide density. In future experiments, we plan to down-substitute the peptides to test the effect of grafting density on liposome binding.

Endosomolysis assay

The peptide identified to bind only to PM-GUVs at pH=7.4 (bLip6) and the two peptides binding to both PM- and LE-GUVs at pH=7.4 and pH=5.5, respectively, (bLips7 and 8) all showed moderate cell uptake. The peptide found to bind only to LE-GUVs at pH = 5.5 did not exhibit cell uptake, fitting with our hypothesis that on-bead binding behavior is related to *in vitro* cell uptake. Closer examination of the fluorescence for bLips6–8 reveals a punctate pattern for all three, with bLip7 and bLip8 also showing a low but diffuse cytosolic background. This could be evident of an altered cell uptake mechanism or instead some degree of endosomal escape, thus was further investigated.

We assayed endosomolytic behavior by testing whether the peptides could improve *in vitro* gene knockdown. Lipofectamine 2000 (LF) was used to deliver GFP antisense siRNA to knockdown GFP protein expression (i.e. green fluorescence) in U87-MG brain tumor cells stably transfected to express GFP. Figure 8 illustrates representative CLSM images of GFP expression for U87-MG cells after incubation with LF only, LF plus GFP antisense siRNA, and LF/siRNA plus bLips7–9. Several representative CLSM images were measured at identical laser settings for each case and their area-normalized fluorescence intensity quantified in ImageJ for statistical comparison (more details found in Supplemental Information). The LF/siRNA control resulted in a decrease in GFP expression to 62% ±13 of the untreated control cells. No significant enhancement of anti-sense activity was seen for bLip7 and bLip8 when compared to the control ($\alpha = 0.05$), However, bLip9 did enhance anti-sense effectiveness when added to cells with the Lipofectamine/siRNA complexes, resulting in a decrease down to 36% ±11. Yet further increase of bLip9 concentration from 20 μM to 50 μM resulted in significant toxicity to the cells.

As a control experiment, we measured the effect of the bLip9 peptide itself on the delivery efficiency of Lipofectamine, given that this may result in an observed increase in gene delivery even in the absence of the presumed endosomolysis. We observed no further knockdown compared to siRNA/LF controls, thus do not expect the bLip9 to artificially enhance siRNA uptake. Although encouraging, the Lipofectamine delivery assay has some weaknesses in the context of measuring peptide delivery in our system. For example, the liposomes comprising Lipofectamine-2000 are highly cationic, both to maximize complexation of anionic siRNA and also to increase extent of cell uptake. Due to this charge

dependence, slight differences in complexation (and therefore internalization) may occur between peptides of varying charge (as tested in this study), which may not correlate well with uptake behavior of the dye-conjugated peptide alone. Furthermore, while the increase in gene delivery associated with bLip9/siRNA/LF co-incubation, and measured lack of knockdown increase for bLip9/siRNA without LF, strongly suggest that complexes are endocytosed and then manage to escape, the precise mechanism of endosomolysis was not determined. Therefore we consider the experimental LF-mediated knockdown evidence to be very preliminary, and in future studies plan to validate the effectiveness of peptide endosomolytic character in more appropriate and relevant *in vivo* nano-delivery platforms, such as upon incorporation into polymeric nanoparticles.

Taken together, these results indicate that the immobilized bead sequential screening methodology can be used as a robust tool to discover, characterize, and compare endosomal escape peptides. Yet peptides found to bind both LE-GUVs and PM-GUVs, while exhibiting CPP character, were not effective in improving gene delivery for our system. An important note is that the bLip peptides were not conjugated to or encapsulated by the Lipofectamine gene delivery vehicles, but rather co-incubated. Therefore, only peptides endocytosed along with Lipofectamine could have a chance to be effective in the endosome. For optimal gene delivery, the bLip peptides will need to be encapsulated into the delivery system, such that maximal target delivery and minimal proteolytic degradation can be achieved.

The results presented here can be expanded in several directions, and we plan to address in more detail the uptake mechanisms of identified bLips, e.g. by chemical or kinetic inhibition of specific endocytic uptake pathways (by sodium azide/2-deoxyglucose, chloroquine/bafilomycin, 4°C cell incubation studies). OBOC libraries can also be further developed by testing peptides ranging from 6–20 amino acids to increase library diversity and better match the range encompassed by reported CPPs/pMAPs. Finally, advances in combinatorial library encoding will soon allow for the quick detection of hundreds of positive hits, e.g. ranked by degree of GUV binding over many conditions, in order to build up peptide motifs necessary and/or sufficient for cell-membrane binding/fusing.

Conclusion

Through sequential combinatorial peptide library screening at appropriate pH with liposomes that mimic the reported lipid/sterol composition of cellular biomembranes, we identified a handful of new peptides with cell uptake or endosomolytic character, which could be correlated with their membrane activity behavior during screening. By employing an OBOC combinatorial library approach, peptide screening can be quickly and easily adapted to a variety of buffer and liposome compositions in order to discover peptides that could be adapted to improve or generate drug delivery scaffolds. We validated that peptide-coated polymer beads able to bind zwitterionic liposomes during screening could reveal peptides that bind to and/or penetrate plasma cell membranes *in vitro*. Furthermore, we found that the best peptide binding “endosomal-type” liposomes (i.e. matching the reported composition of late endosomal lipids and cholesterol) at pH 5.5, could enhance the antisense ability of an siRNA/Lipofectamine gene delivery system to knockdown GFP expression in U87-MG brain tumor cells. We believe that the variety of potential peptides to be

discovered, and the ease of the methodology to find them, renders this technique as a breakthrough for bioengineering drug delivery scaffold design.

Supplementary Material

Refer to Web version on PubMed Central for supplementary material.

Acknowledgments

R.P.C. would like to acknowledge support from the NIH T32 HL007013 training grant. This work is also supported in part by NIH CA115483 awarded to K.S.L.

Abbreviations

MAPs	membrane active peptides
pMAPs	pH-dependent membrane active peptides
CPPs	cell-penetrating peptides
GUV	giant unilamellar vesicle
PEG	polyethylene glycol
TAMRA	5-Carboxytetramethylrhodamine
PM	plasma membrane
LE	late endosome
R9	nona-arginine
DAPI	4’,6-diamidino-2-phenylindole
PI	propidium iodide
OBOC	one-bead-one-compound
CLSM	confocal laser scanning microscopy
bLip	liposome binding peptide

References

1. Lehner R, Wang X, Marsch S, Hunziker P. Intelligent nanomaterials for medicine: Carrier platforms and targeting strategies in the context of clinical application. Nanomed-Nanotechnol. 2013; 9:742–757.
2. Liang, W., W Lam, JK. Molecular Regulation of Endocytosis. Ceresa, B., editor. Vol. Chapter 17. InTech; 2012.
3. Hillaireau H, Couvreur P. Nanocarriers’ entry into the cell: relevance to drug delivery. Cell. Mol. Life Sci. 2009:2873–2896. [PubMed: 19499185]
4. Last NB, Schlamadinger DE, Miranker AD. A common landscape for membrane-active peptides. Protein Sci. 2013; 22:870–882. [PubMed: 23649542]

5. Gautam A, Singh H, Tyagi A, Chaudhary K, Kumar R, Kapoor P, Raghava GPS. CPPsite: a curated database of cell penetrating peptides. Database. 2012; 2012:bas015–bas015. [PubMed: 22403286]
6. Munyendo WL, Lv H, Benza-Ingoula H, Baraza LD, Zhou J. Cell Penetrating Peptides in the Delivery of Biopharmaceuticals. Biomolecules. 2012; 2:187–202. [PubMed: 24970133]
7. Martín I, Teixidó M, Giralt E. Design, Synthesis and Characterization of a New Anionic Cell-Penetrating Peptide: SAP(E). ChemBioChem. 2011; 12:896–903. [PubMed: 21365733]
8. Yamada T, Das Gupta TK, Beattie CW. p28, an Anionic Cell-Penetrating Peptide, Increases the Activity of Wild Type and Mutated p53 without Altering Its Conformation. Mol Pharm. 2013; 10:3375–3383. [PubMed: 23952735]
9. Wiedman G, Wimley WC, Hristova K. Testing the limits of rational design by engineering pH sensitivity into membrane-active peptides. BBA-Biomembranes. 2015; 1848:951–957. [PubMed: 25572997]
10. Sela M, Zisman E. Different roles of D-amino acids in immune phenomena. FASEB J. 1997; 11:449–456. [PubMed: 9194525]
11. Marks JR, Placone J, Hristova K, Wimley WC. Spontaneous Membrane-Translocating Peptides by Orthogonal High-Throughput Screening. J. Am. Chem. Soc. 2011; 133:8995–9004. [PubMed: 21545169]
12. Blondelle SE, Houghten RA, Pérez Payá E. Identification of Inhibitors of Melittin Using Nonsupport-bound Combinatorial Libraries. J. Biol. Chem. 1996; 271:4093–4099. [PubMed: 8626746]
13. Blondelle SE, Houghten RA, Pérez Payá E. All D-amino acid hexapeptide inhibitors of melittin's cytolytic activity derived from synthetic combinatorial libraries. J. Mol. Recognit. 1996; 9:163–168. [PubMed: 8877809]
14. Chen X, Gambhir SS. Significance of one-bead-one-compound combinational chemistry. Nat. Chem. Biol. 2006; 2:351–352. [PubMed: 16783336]
15. Xiao W, Wang Y, Lau EY, Luo J, Yao N, Shi C, Meza L, Tseng H, Maeda Y, Kumaresan P, Liu R, Lightstone FC, Takada Y, Lam KS. The Use of One-Bead One-Compound Combinatorial Library Technology to Discover High-Affinity alpha-v-beta-3 Integrin and Cancer Targeting Arginine-Glycine-Aspartic Acid Ligands with a Built-in Handle. Mol. Cancer Ther. 2010; 9:2714–2723. [PubMed: 20858725]
16. Fuchs SM, Raines RT. Pathway for polyarginine entry into mammalian cells. Biochemistry. 2004; 43:2438–2444. [PubMed: 14992581]
17. Pujals S, Giralt E. Proline-rich, amphipathic cell-penetrating peptides. Adv. Drug Deliver. Rev. 2008; 60:473–484.
18. Maiolo JR, Ferrer M, Ottinger EA. Effects of cargo molecules on the cellular uptake of arginine-rich cell-penetrating peptides. Biochim. Biophys. Acta. 2005; 1712:161–172. [PubMed: 15935328]
19. van Meer G, Voelker DR, Feigenson GW. Membrane lipids: where they are and how they behave. Nat. Rev. Mol. Cell Bio. 2008; 9:112–124. [PubMed: 18216768]

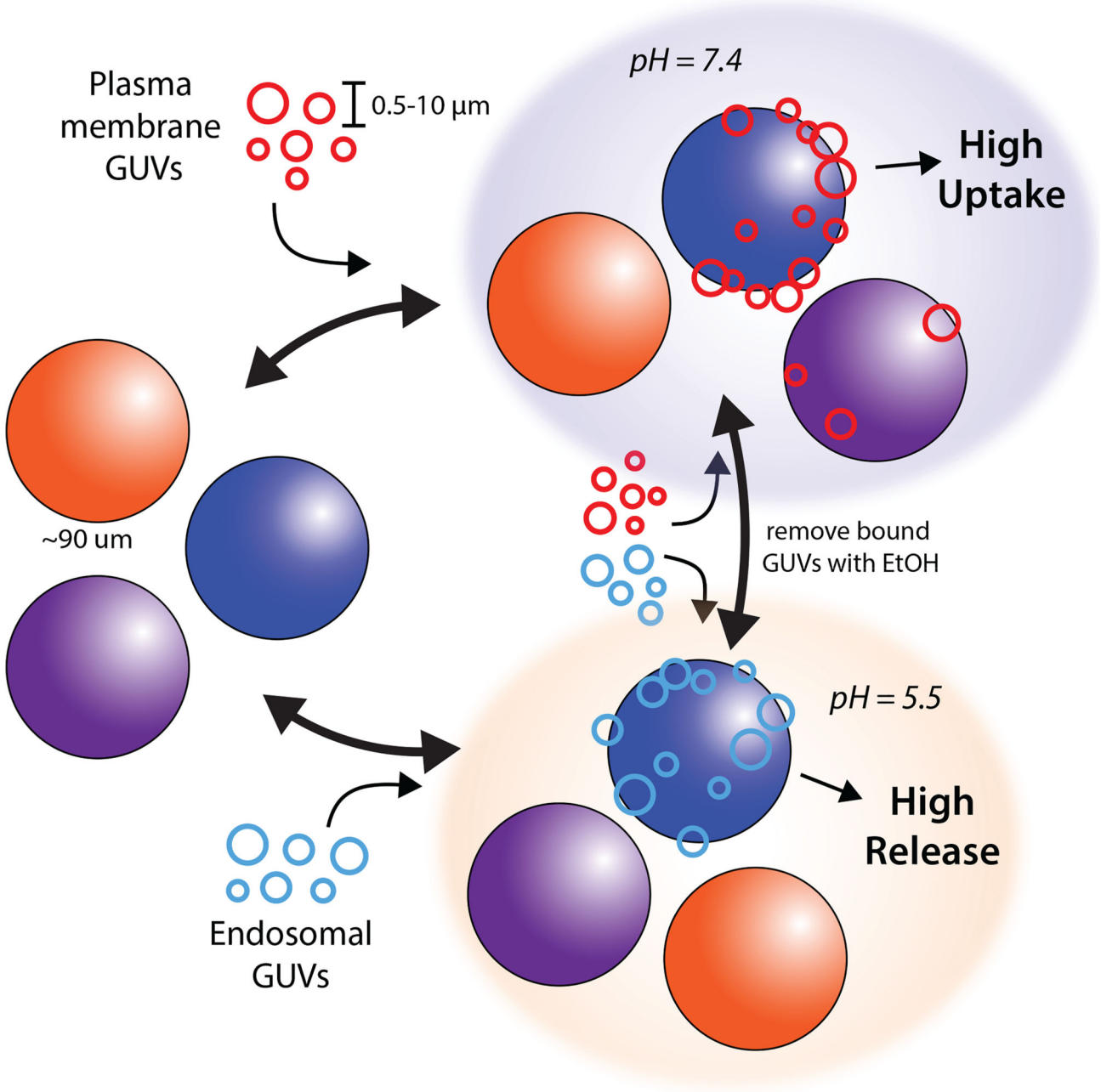

Figure 1.

Sequential OBOC Screening Scheme. Beads from an OBOC combinatorial peptide library are immobilized on a planar polystyrene surface before incubation with fluorescently-labeled giant unilamellar vesicles (GUVs). The library can be washed with ethanol to remove bound GUVs for quick re-screening of the same beads under various conditions such as GUV composition and pH. More than 200,000 beads can be scanned within 20 minutes by automating a confocal microscopy tile-scan program. Beads are individually ranked for changes in fluorescence intensity over time due to binding of fluorescently-labeled GUVs, and subsequently compared across screening conditions.

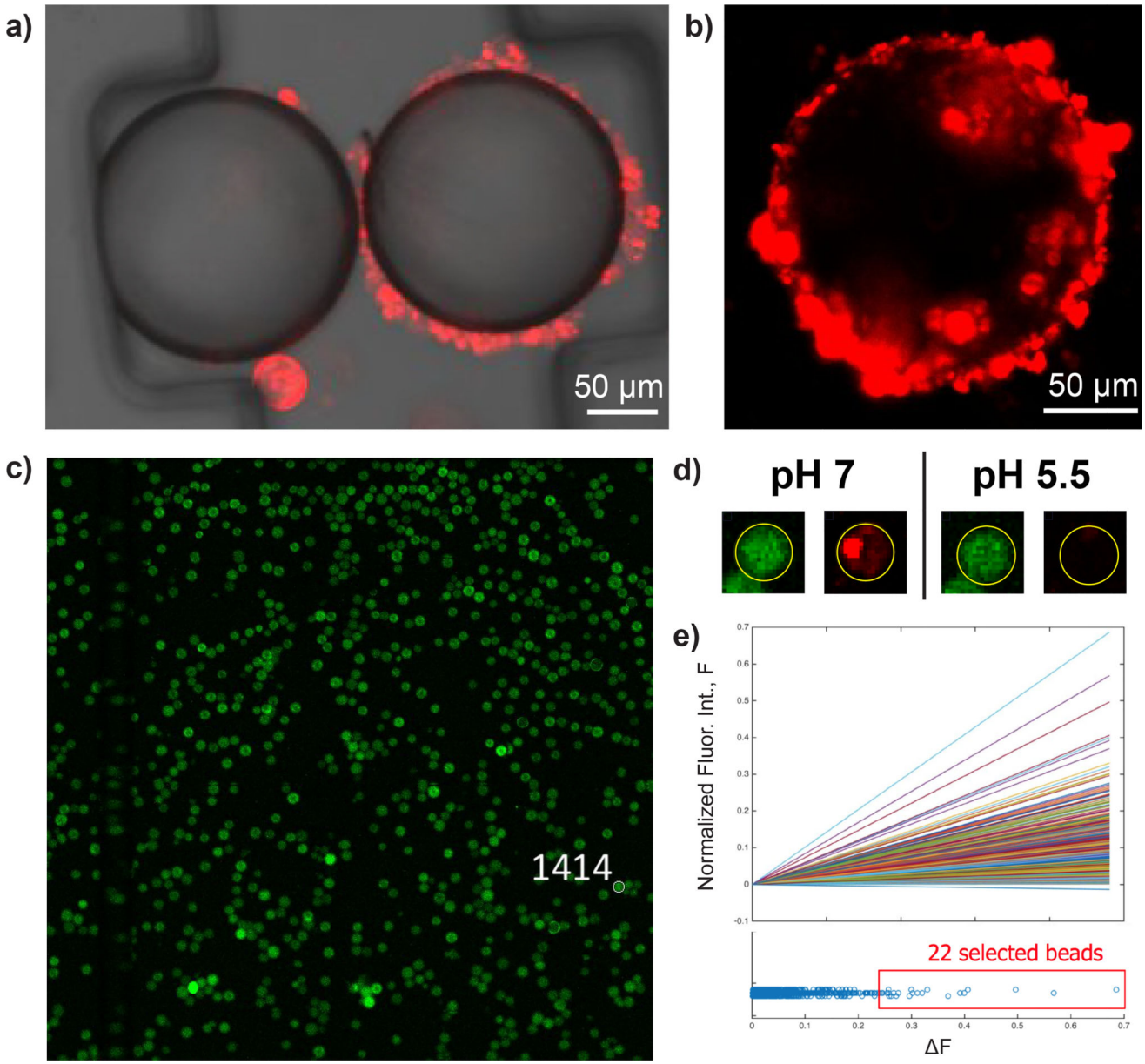

Figure 2.

Detection and selection scheme. (a) CLSM overlay of transmitted light (polymer beads) and red fluorescence channel (GUVs) during a typical screening. Beads that bind many GUVs (*right*) are selected as peptides of interest while non-binding beads (*left*) are ignored. (b) Red fluorescence channel CLSM image with GUV curvature evident. (c) Each bead's autofluorescence signal (green channel) is used to spatially map out hundreds of thousands of beads in a single polystyrene dish. (d) An automated program can identify specific beads (e.g. bead 1414 pictured in (c)) based on discrimination of change in fluorescence over time. (e) The top several beads can be quickly picked and sequenced for further investigation.

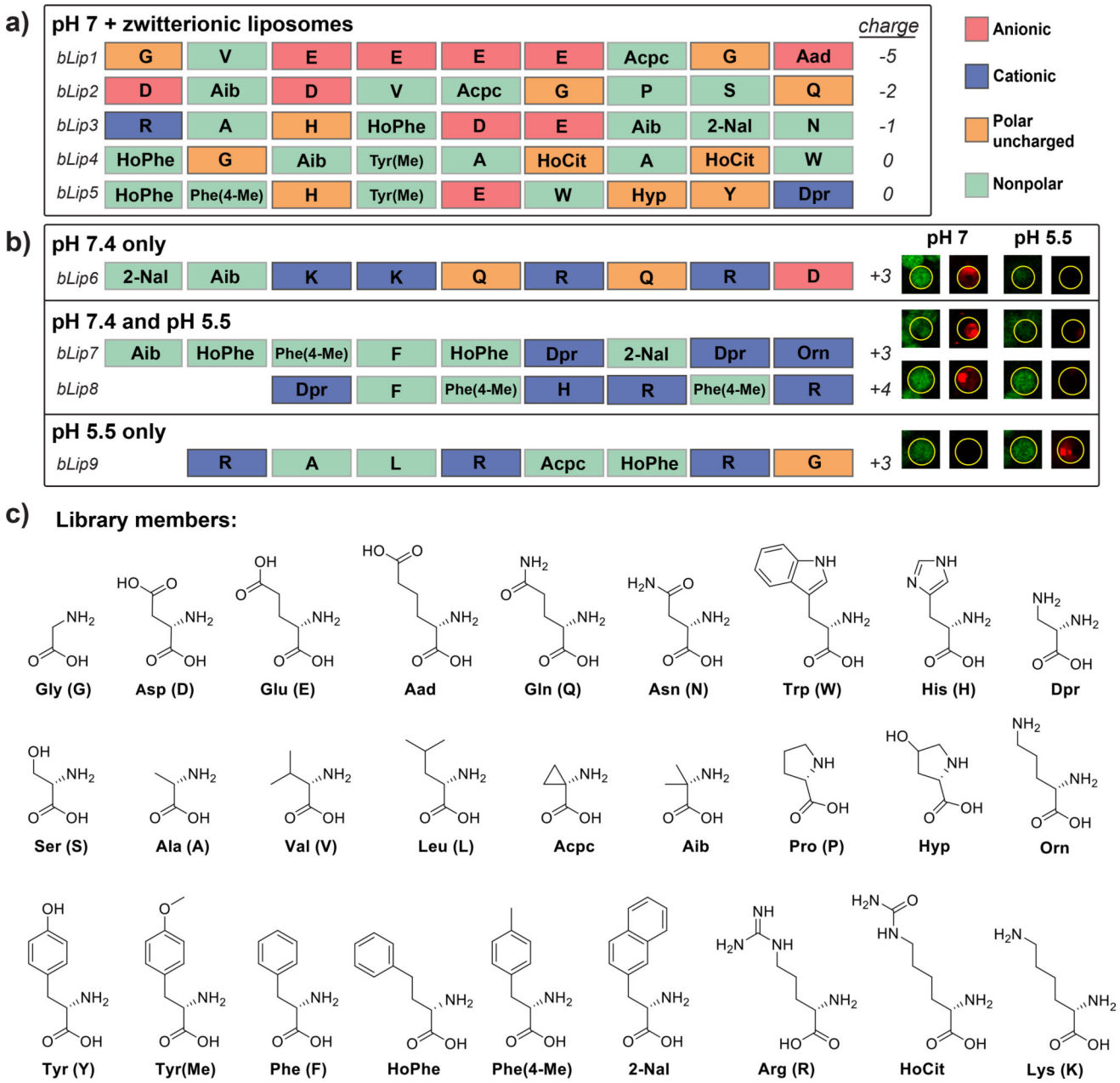

Figure 3.

Screening results and peptide library components. (a) Peptide sequences for five positive hits (termed bLips1–5) isolated after three screening rounds for binding simple fluorophore-labeled zwitterionic GUVs. (b) Peptide sequences identified with a more advanced screening methodology, which tracks each bead's binding to either plasma membrane type or endosomal type GUVs at appropriate pH. (c) Amino acid abbreviations and corresponding side-chain functional groups comprising the combinatorial library screened in this study. Unnatural residues are blue.

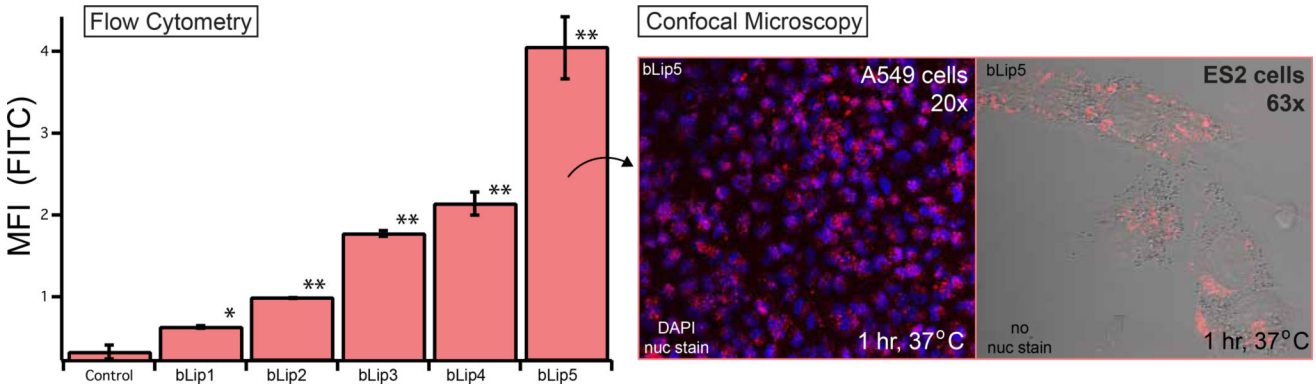

Figure 4.

In vitro uptake of bLips1–5 measured by confocal microscopy. (a) Flow cytometry measurement of mean fluorescence intensity (MFI) for A549 cells after incubation with FITC-labeled bLips for 3 h. (b) *Left* : CLSM fluorescence image illustrating TAMRA-conjugated bLip5 uptake in A549 lung cancer cells (blue channel-DAPI nuclear stain) *Right*: Higher magnification red fluorescence and transmitted light overlay CLSM image showing cellular localization of bLip5 in ES2 ovarian cancer cells.

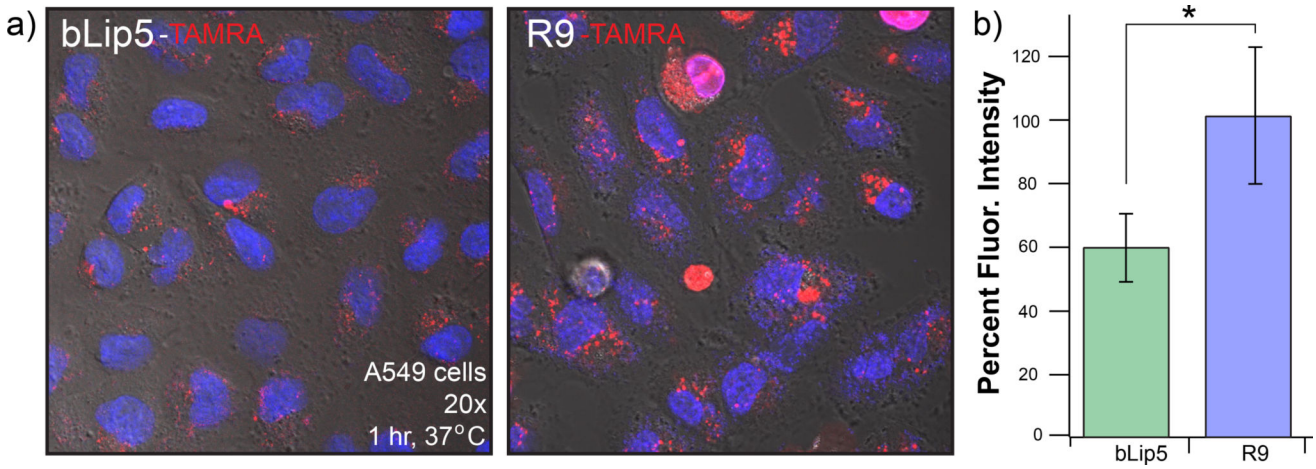

Figure 5.

(a) CLSM overlay of brightfield (cells) blue fluorescence channel (nuclei stain), and red fluorescence channel (TAMRA dye) following cell uptake of either bLip5-TAMRA (*left*) or R9-TAMRA (*right*). (b) Representative CLSM images were analyzed for fluorescence intensity normalized by cell area. The bLip5-TAMRA intensity is graphed as percent fluorescent intensity compared to R9-TAMRA. Error bars represent one standard deviation.

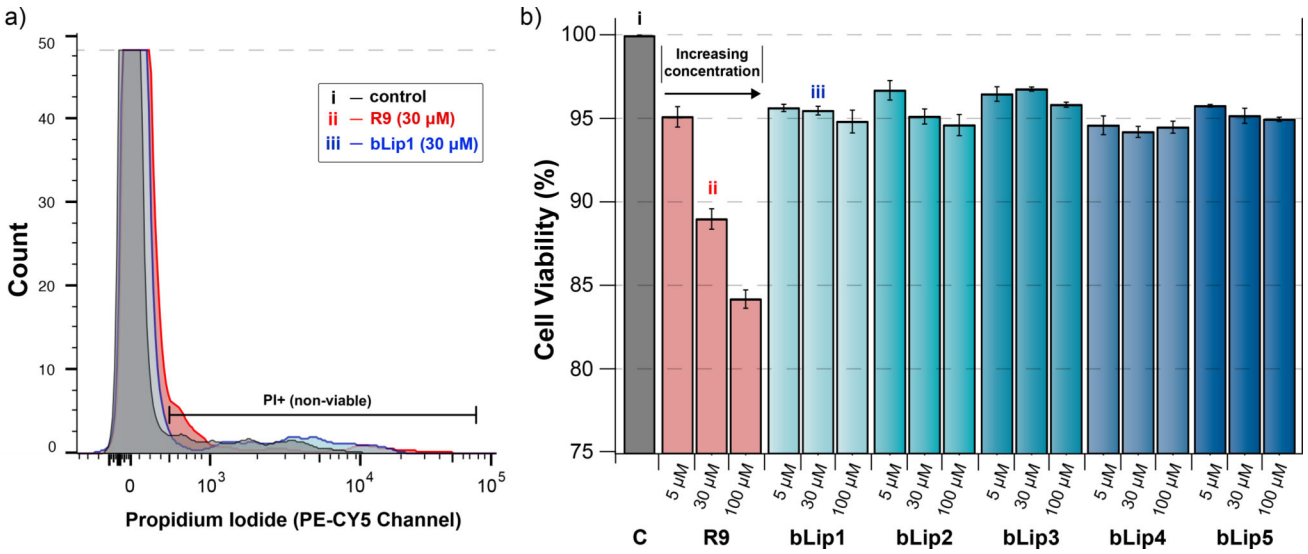

Figure 6.

Toxicity of bLips measured by flow cytometry. (a) Representative flow cytometry raw fluorescence traces following propidium iodide addition for (i) A549 control cells (no peptide added), and A549 cells incubated with (ii) 30 μM R9, and (iii) 30 μM bLip1. (b) Percentage of viable A549 cells based on PI viability assay for R9 and the five peptide bLips at increasing concentration of 5, 30, and 100 μM (roman numerals indicate the data set referenced in *(a)*). The bLips show very little cytotoxicity, even at high concentration. C stands for control.

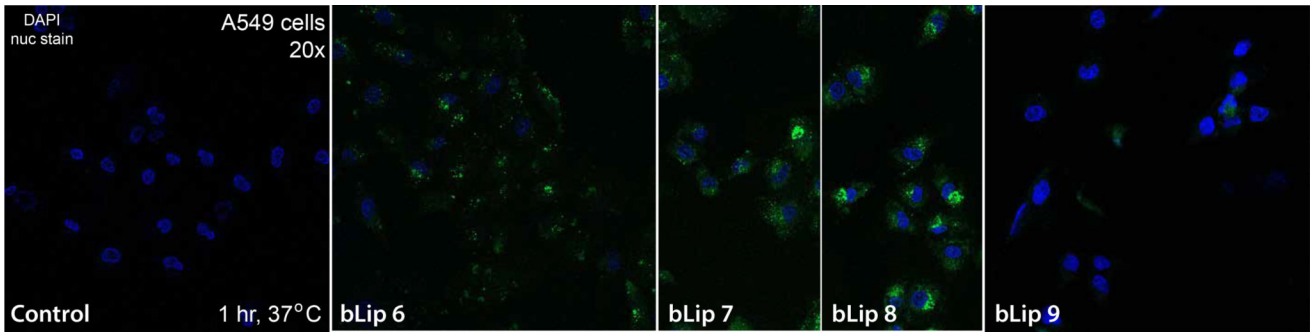

Figure 7.

In vitro uptake of bLips6–9 measured by confocal microscopy. CLSM fluorescence image illustrating FITC-conjugated bLips6–9 uptake in A549 lung cancer cells (blue channel-DAPI nuclear stain) after 1 h incubation. bLips6–9 (identified to bind PM-GUVs at pH = 7.4) primarily showed punctate fluorescence indicative of endocytosis, while bLip 9 (binding only LE-GUVs at pH = 5.5) did not exhibit cell penetration.

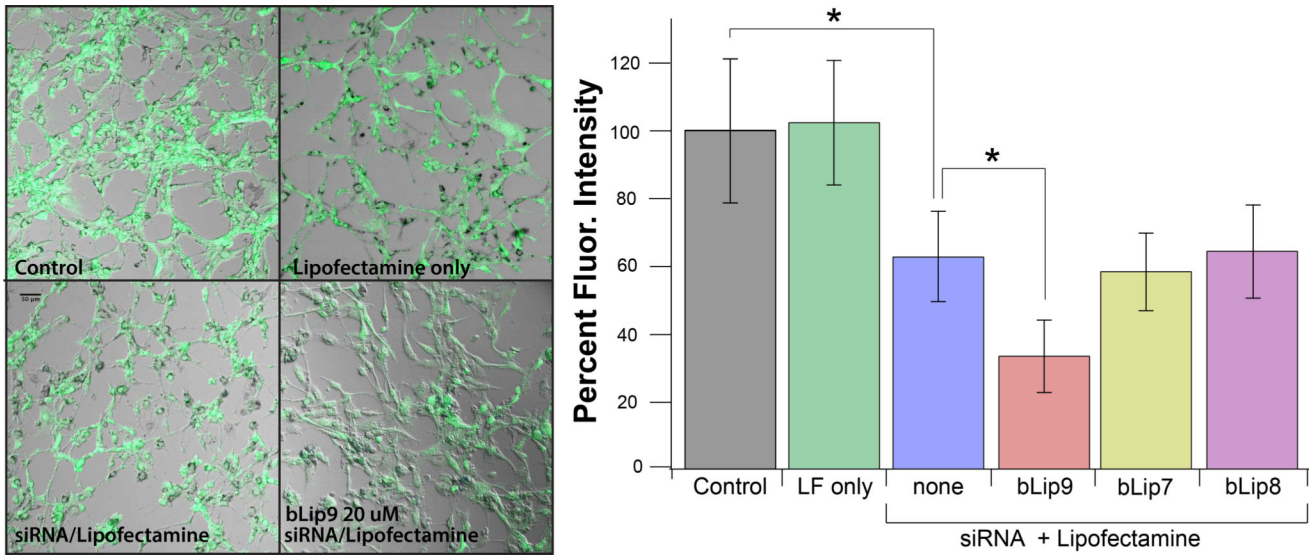

Figure 8.

In vitro GFP knockdown for peptides binding to LE-GUVs at pH = 5.5. CLSM micrographs were used to quantify GFP expression in U87-MG brain tumor cells, 72 h post treatment. For each case, several representative images were analyzed for fluorescence intensity (normalized by cell area). The average intensities are graphed as percent GFP expression compared to control (no treatment). Error bars represent one standard deviation. The combination of GFP-antisense-siRNA and Lipofectamine resulted in significant decrease in GFP expression (α = 0.05) compared to control or Lipofectamine only (LF only). When bLip9 was co-incubated at 20 μM with siRNA/Lipofectamine complexes, GFP expression was further decreased. At 20 μM, bLips7 and 8 did not significantly decrease GFP expression.